Evolving Hemodynamics in Fontan Circulation: Age-Driven Insights in Patients with Interrupted Inferior Vena Cava and Hepatoazygos Shunt

Vikas Kannojiya PhD[1,4], Akshita Sahni MS[1], Emily Eickhoff MEngg[1], Neha Zacharia[1], Nicole. St. Clair BS[1], Noah Schulz MS[1], Peter E. Hammer PhD[1,4], Pedro J. del Nido MD[1,2], Rahul H. Rathod MD MBA[2,3] David M. Hoganson MD[1,4], and Vijay Govindarajan PhD*[1,4,5]

[1]Department of Cardiovascular Surgery, Boston Children's Hospital, Boston, MA, [2]Department of Cardiology, Boston Children's Hospital, Boston, MA, [3]Department of Pediatrics, Harvard Medical School, Boston, MA, [4]Department of Surgery, Harvard Medical School, Boston, MA, [5]Department of Internal Medicine, The University of Texas Health Science Center at Houston

Supplementary Materials

Address of Correspondence

Email: Vijay.govindarajan@childrens.harvard.edu

Vijay Govindarajan, PhD

Department of Cardiovascular Surgery

Boston Children's Hospital

300 Longwood Avenue

Boston, MA 02115

Supplementary Tables

Table S1: Summary of patient-specific clinical data utilized in the study, including key parameters essential for modeling and analysis of flow dynamics and physiological conditions. Here, Dao: Descending aorta, LSVC: Left superior vena cava, RSVC: Right superior vena cava, LPA: Left pulmonary artery, RPA: Right pulmonary artery, BSA: Body surface area, F: Female, M: Male, and Arteriovenous Malformations.

	MRI Measured Inflow (L/min)			MRI Measured Outflow (L/min)		BSA	Age (Years)	Sex	AVM
Patient	DAo	LSVC	RSVC	LPA	RPA				
1	2.76	0.92	0.92	1.43	1.93	1.66	18.9	F	Yes
2	3.1	1.4	1.4	2.54	2.91	1.08	10.4	F	Yes
3	2.9	0.38	0.58	1.8	1.7	1.16	13.4	F	Yes
4	1.99	0.47	0.47	0.47	0.47	1.69	21	F	Yes
5	4.5	0.765	0.765	17 mmHg*	16 mmHg*	1.52	14.9	M	Yes
6	5.72	1.045	1.045	3.7	3.8	1.5**	17.9	M	Yes
7	2.3	0.75	0.5	1	2.2	1.5**	8	M	Yes
8	1.0395	0.594	0.594	14 mmHg*	15mmHg*	0.66	4.5	N/A	No
9	1.04	0.6	1.48	1.44	0.83	0.679	5.42	M	No
10	3.8	2.435***	2.435***	1.95	3.85	1.626	18.76	M	Yes
11	1.19	0.905***	0.905***	0.94	1.08	0.690	5.17	M	No
12	0.4	1.5	0.5	0.9	1.1	0.727	4.17	F	N/A
13	0.9	1***	1***	0.6	2.2	0.667	3.75	F	N/A
14	1.03	1.28***	1.28***	2.55	0.92	0.765	5.84	F	N/A
15	1.36	1.08	2.01	0.98	1.35	0.839	5.59	M	N/A
16	3.1	0.5	1	1.4	2.6	1.607	24.77	F	N/A
17	3.5	0.9	1.6	1.9	2.5	1.719	21.1	F	N/A

Assumptions: *In the absence of specific split values for the LPA and right pulmonary artery RPA from the MRI report, for Patient 5, the flow split between the LPA and RPA was calculated based on the pressures at the respective outlets (LPA: 17 mmHg and RPA: 16 mm Hg, as per the Cath report). The total body flow was distributed according to the ratio of the pressures at the LPA and RPA outlets, assuming that flow resistance is inversely proportional to the pressure at each outlet reflecting the vascular resistance. For patient 8, the pulmonary vascular resistance (PVR) of 1.1 indexed Wood units (equivalent to 5.79×10^{6} Pa·s·m^{-3}) provided in the Cath report for Patient 8 was used. **BSA values for patients 6 and 7 were estimated based on the upper-to-lower body flow ratios reported in the MRI. Specifically, a BSA of 0.5 was assigned for a ratio of 2, a BSA of 1 for a ratio of 1, and a BSA of 1.5 for a ratio of 0.5. *** The flow measured at the SVC was evenly divided between the LSVC and RSVC.

Table S2: Shaprio-Wilk test for normality of PL, VDR, and VOR distribution corresponding to each body flow ratio. Here a P-Value > 0.05 indicates normal distribution.

Shaprio-Wilk Test				
Upper: Lower Body Flow = 2				
	Mean	SD	Statistics	P-Value
PL	18.8118	25.3245	0.7228	0.0002123

VDR	0.002395	0.002338	0.8137	0.003147
VOR	0.003646	**0.002009**	0.9429	0.3546
Upper: Lower Body Flow = 1				
PL	49.6159	63.8686	0.76	0.0006029
VDR	0.007586	0.006661	0.8714	0.02309
VOR	0.007235	0.00338	0.9113	0.1054
Upper: Lower Body Flow = 0.5				
PL	119.4	169.3213	0.6694	0.00005308
VDR	0.01757	0.01796	0.8092	0.00272
VOR	0.01123	0.005598	0.8986	0.06436

Supplementary Figures

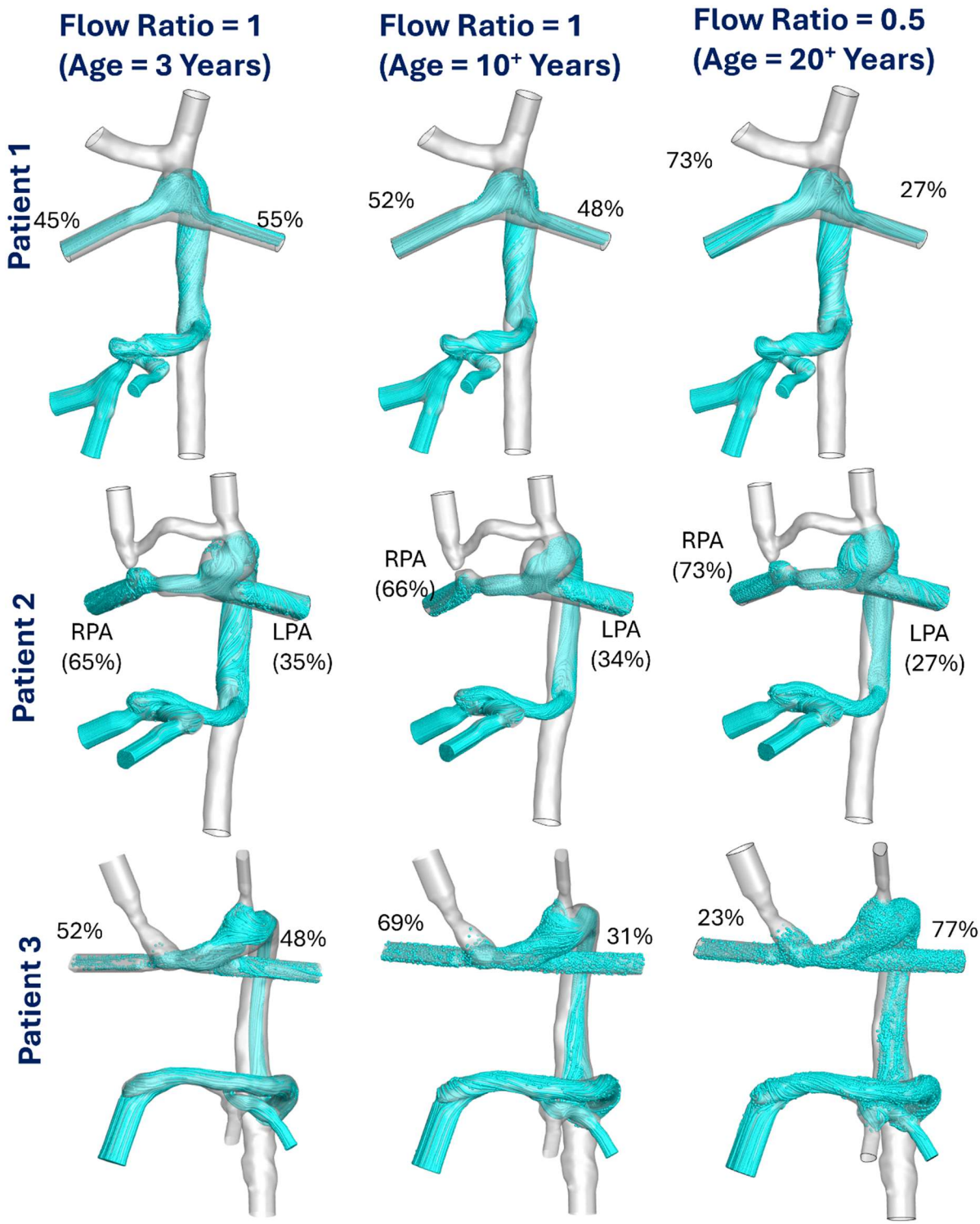

Figure S1.1 Variation of Hepatic Distribution with age-related changes in upper-to-lower body flow ratios for different patients

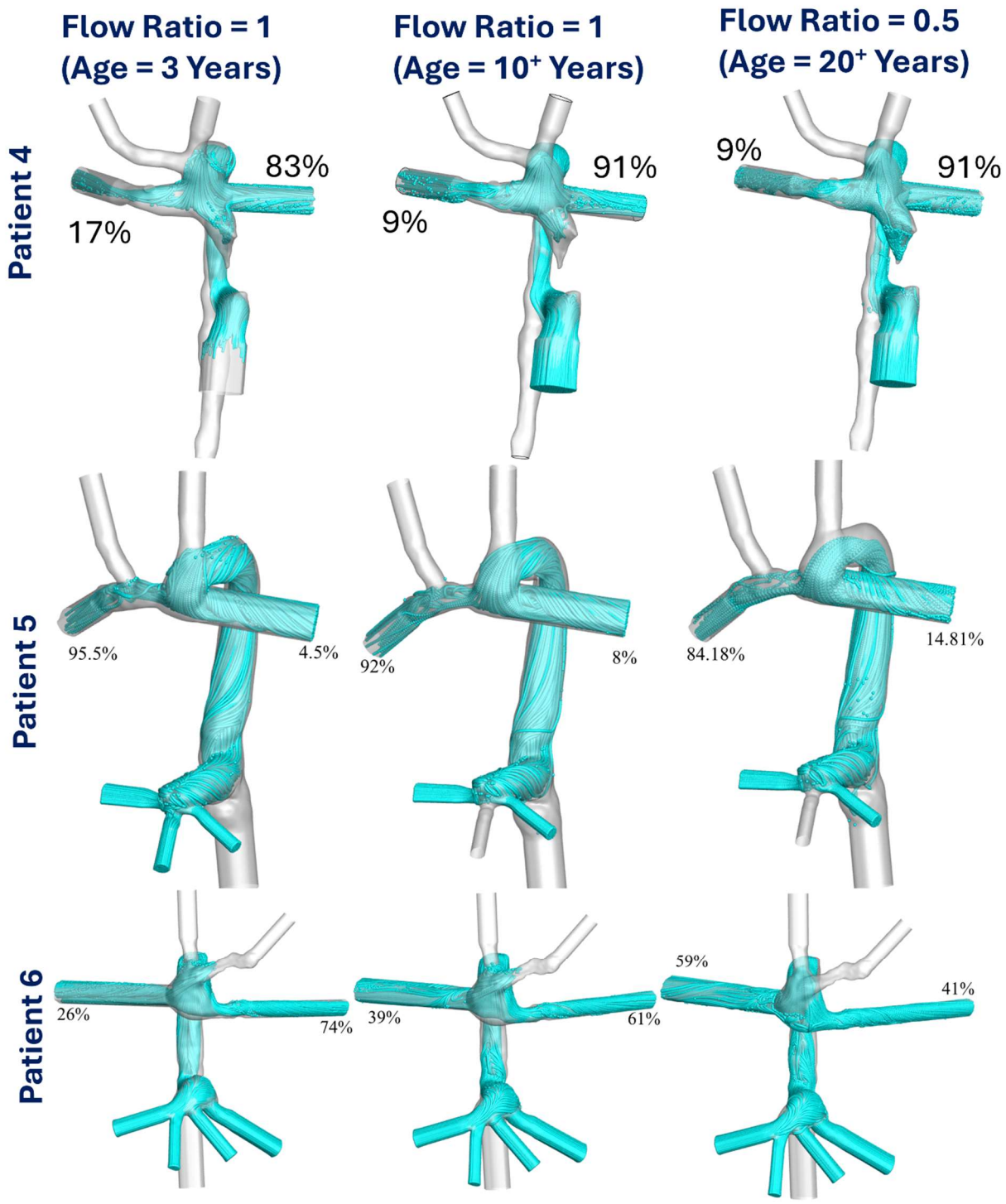

Figure S1.2 Variation of Hepatic Distribution with age-related changes in upper-to-lower body flow ratios for different patients

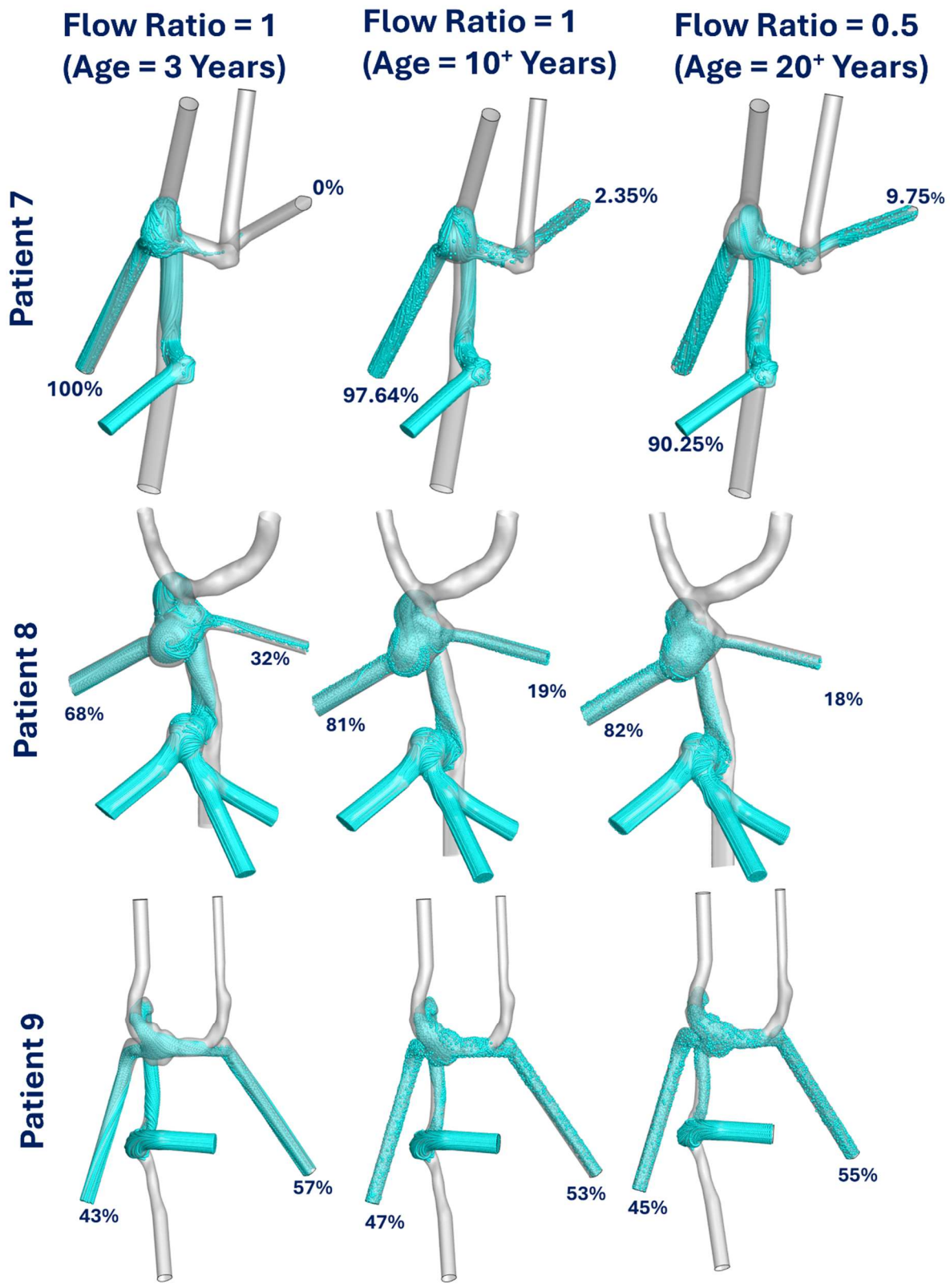

Figure S1.3 Variation of Hepatic Distribution with age-related changes in upper-to-lower body flow ratios for different patients

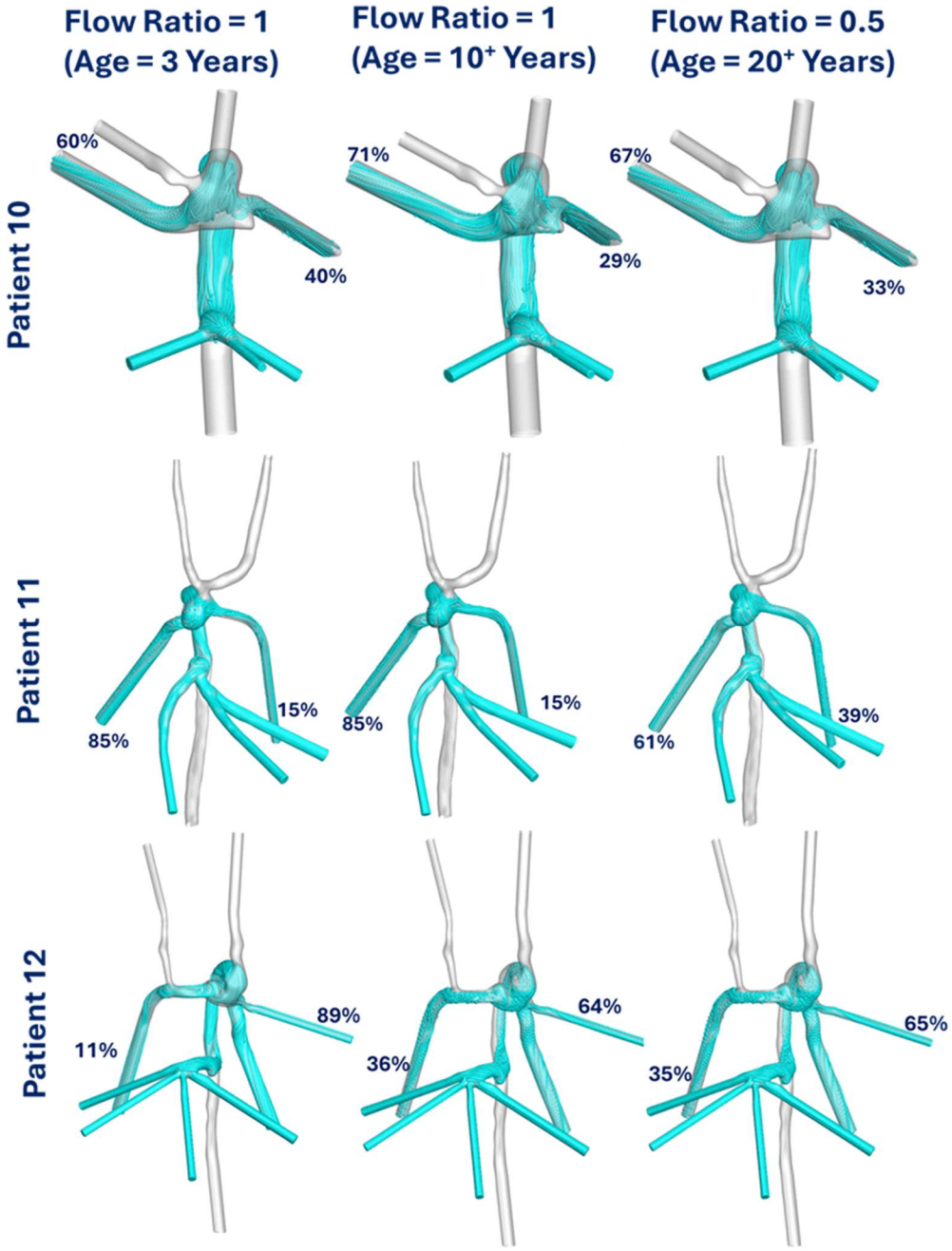

Figure S1.4 Variation of Hepatic Distribution with age-related changes in upper-to-lower body flow ratios for different patients

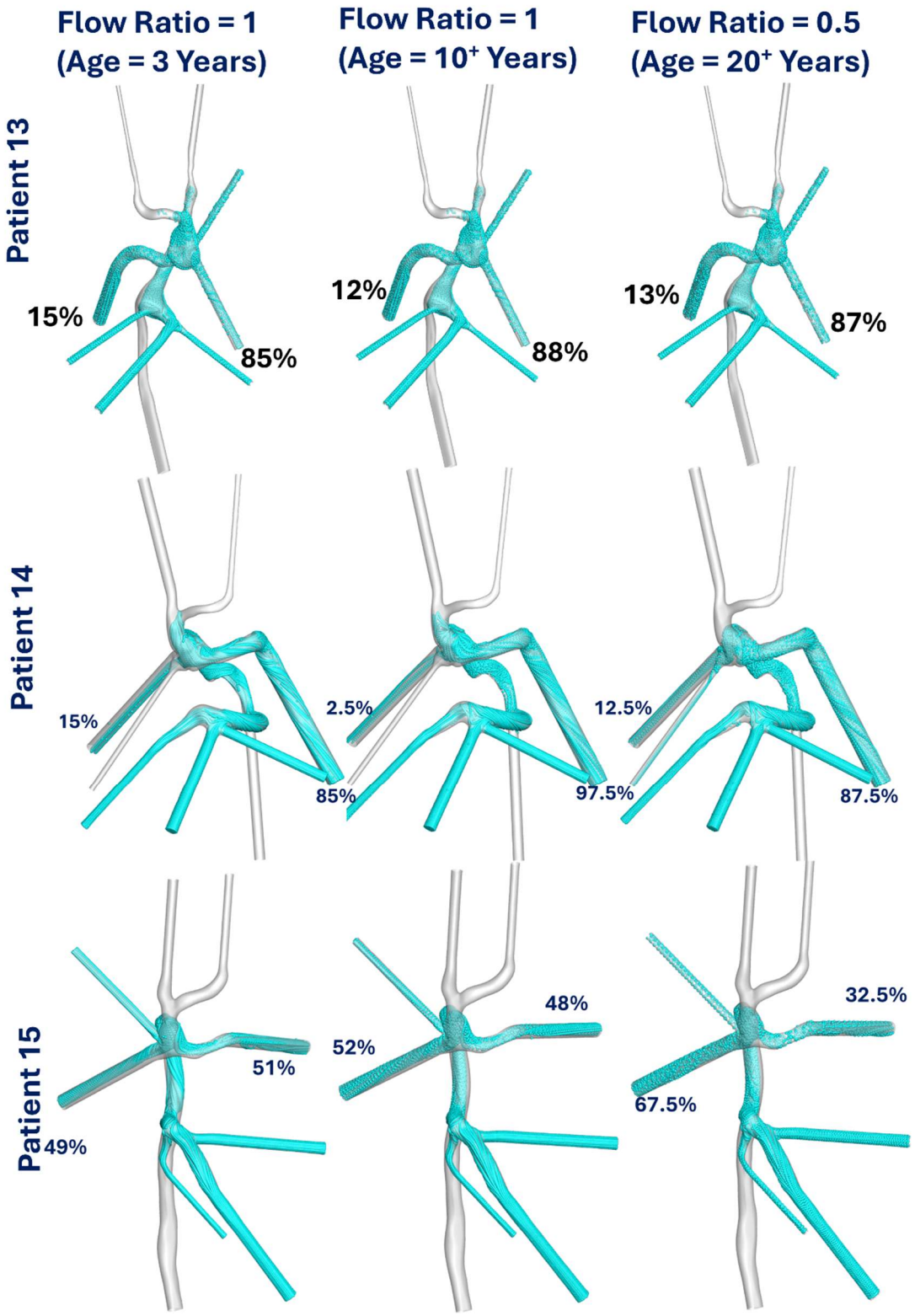

Figure S1.5 Variation of Hepatic Distribution with age-related changes in upper-to-lower body flow ratios for different patients

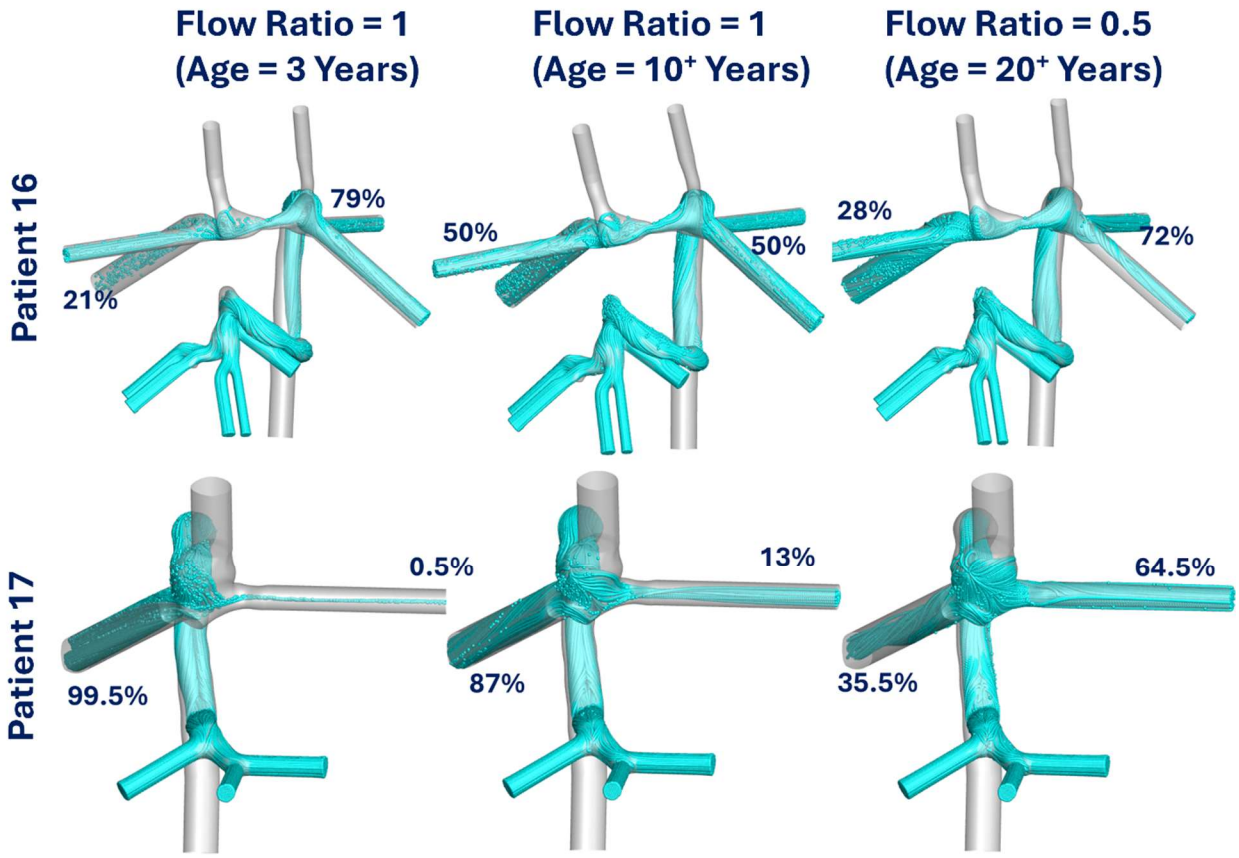

Figure S1.6 Variation of Hepatic Distribution with age-related changes in upper-to-lower body flow ratios for different patients

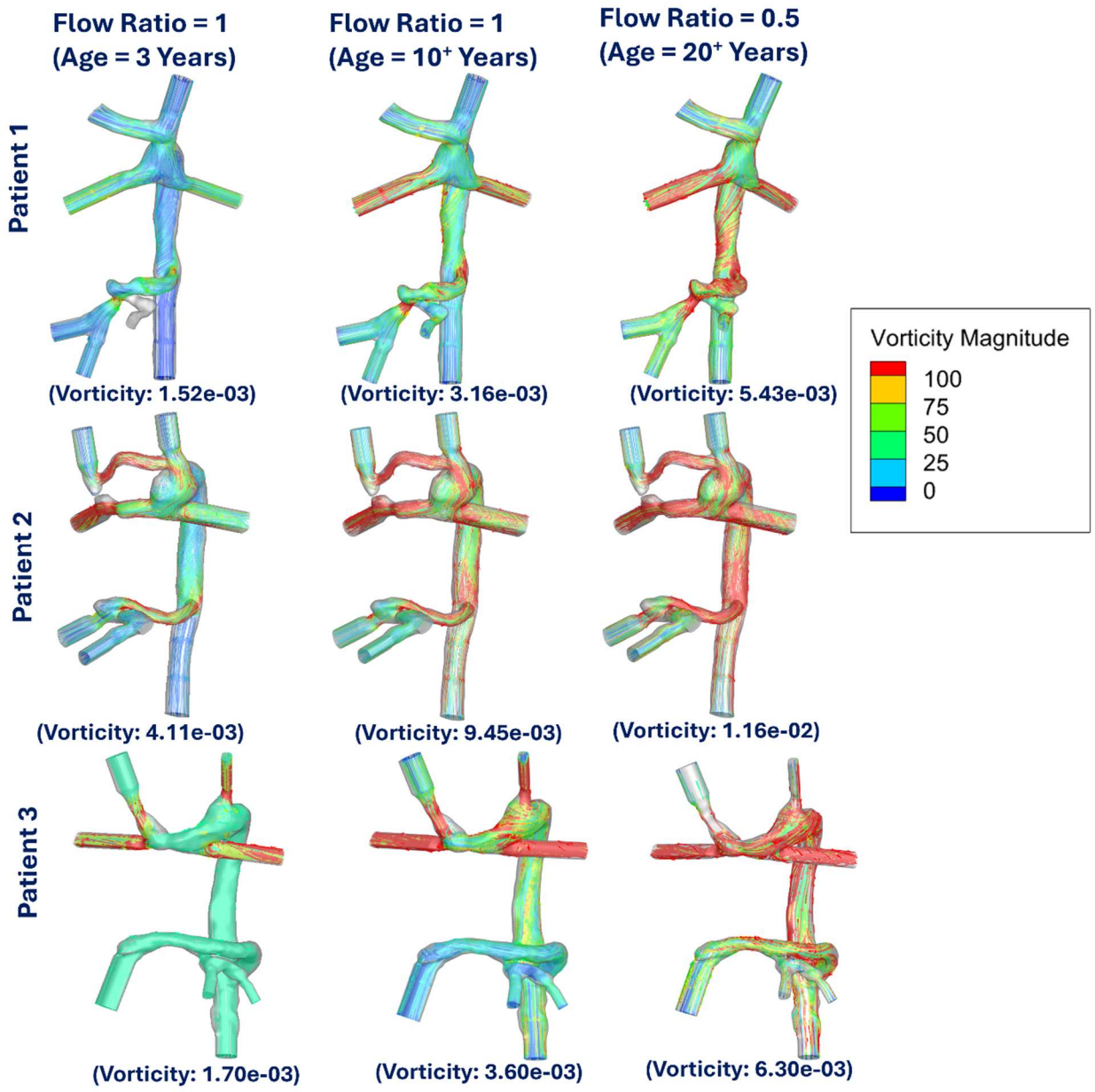

Figure S2.1 Age-related spatial variation of Vorticity with upper-to-lower body flow ratios for different patients, with corresponding value of integrated vorticity.

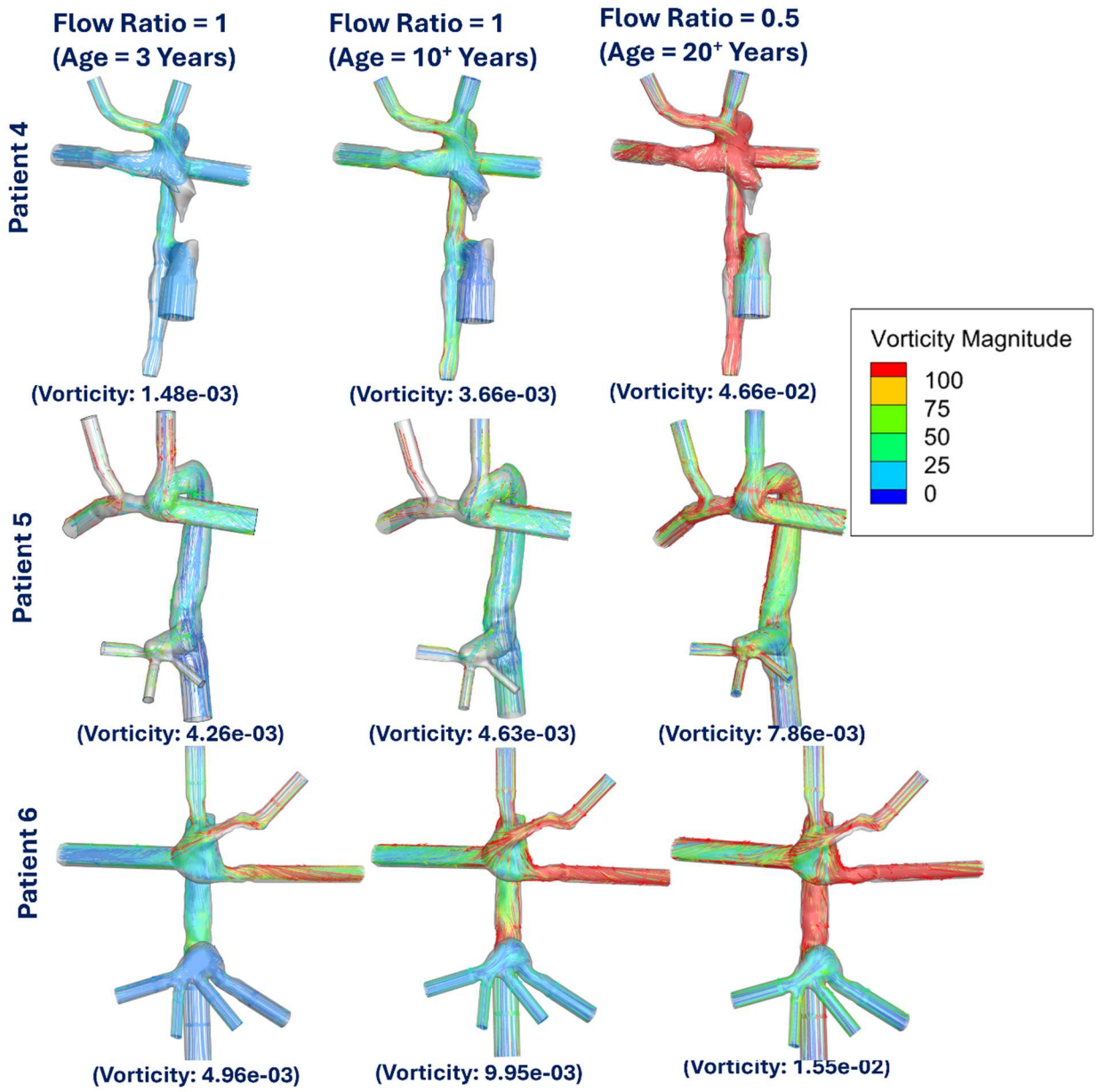

Figure S2.2 Age-related spatial variation of Vorticity with upper-to-lower body flow ratios for different patients, with corresponding value of integrated vorticity.

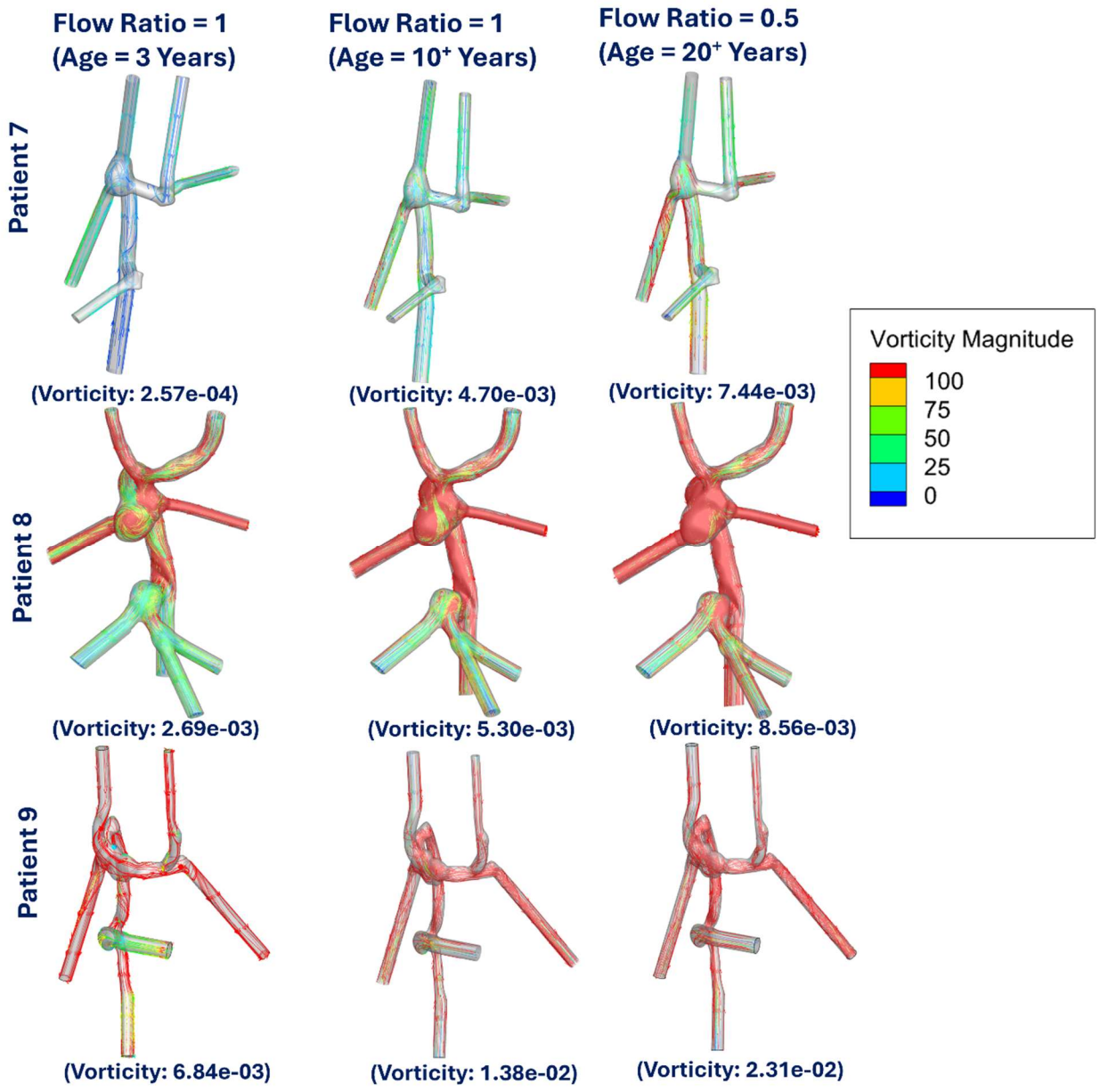

Figure S2.3 Age-related spatial variation of Vorticity with upper-to-lower body flow ratios for different patients, with corresponding value of integrated vorticity.

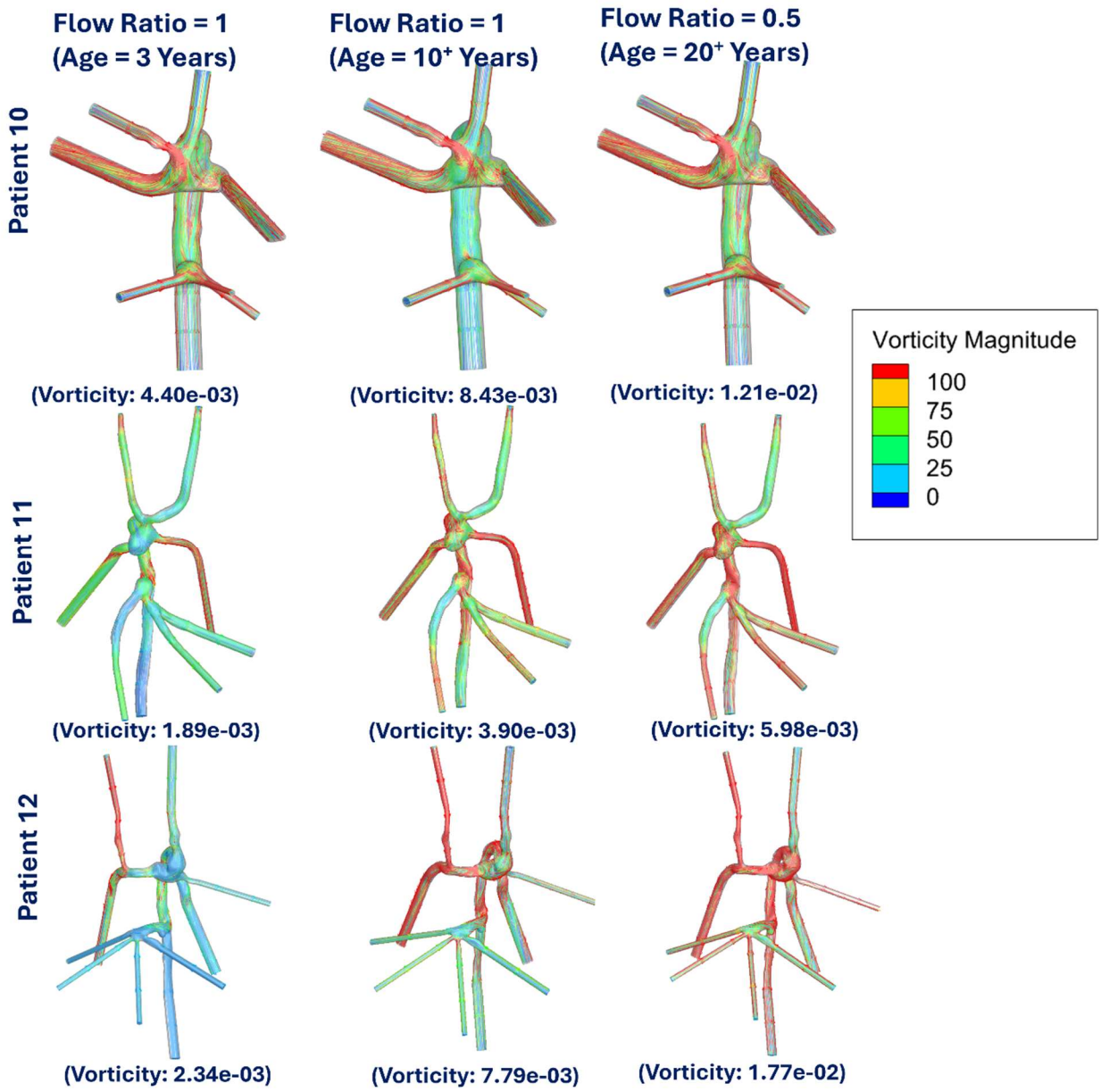

Figure S2.4 Age-related spatial variation of Vorticity with upper-to-lower body flow ratios for different patients, with corresponding value of integrated vorticity.

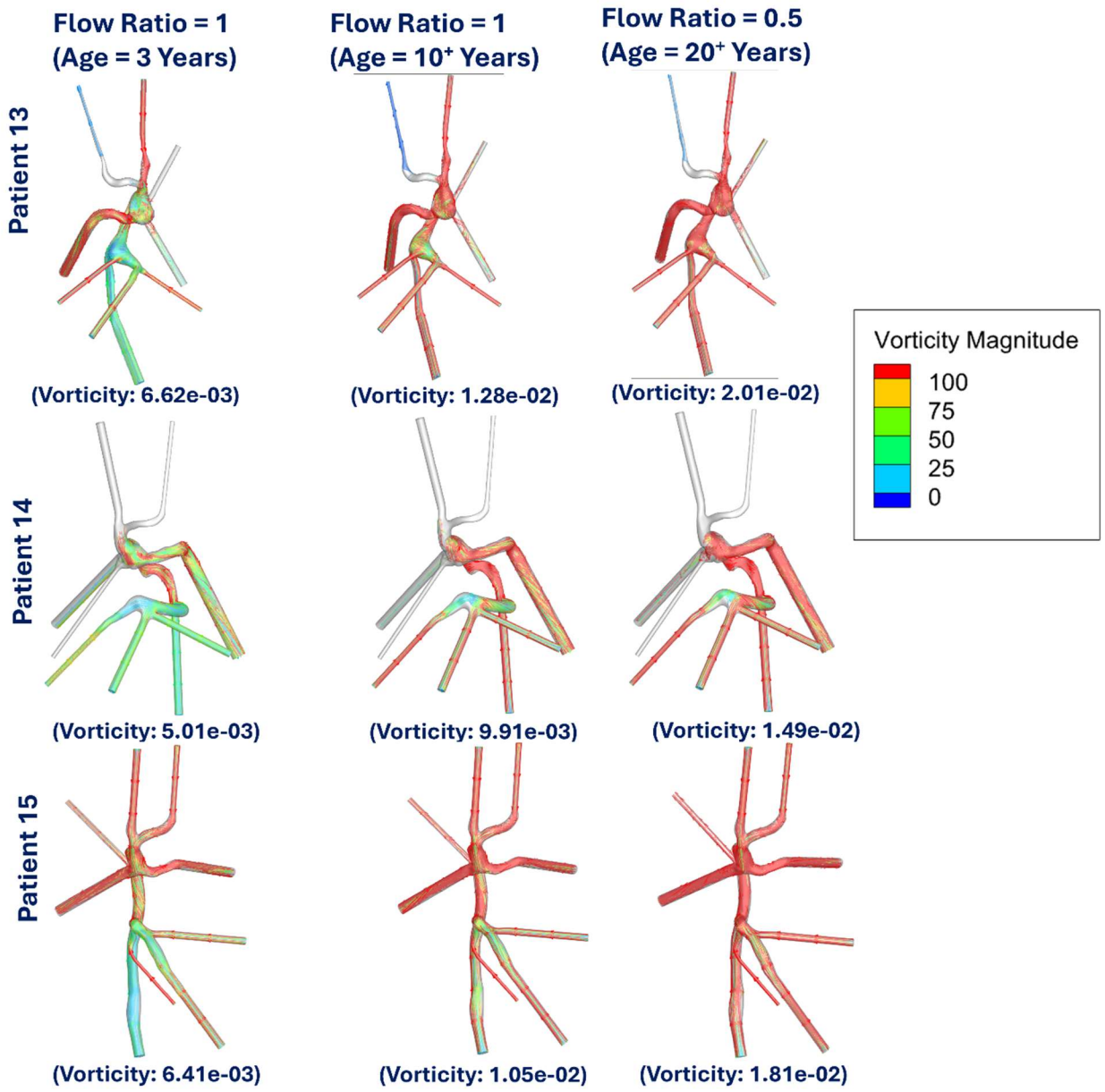

Figure S2.5 Age-related spatial variation of Vorticity with upper-to-lower body flow ratios for different patients, with corresponding value of integrated vorticity.

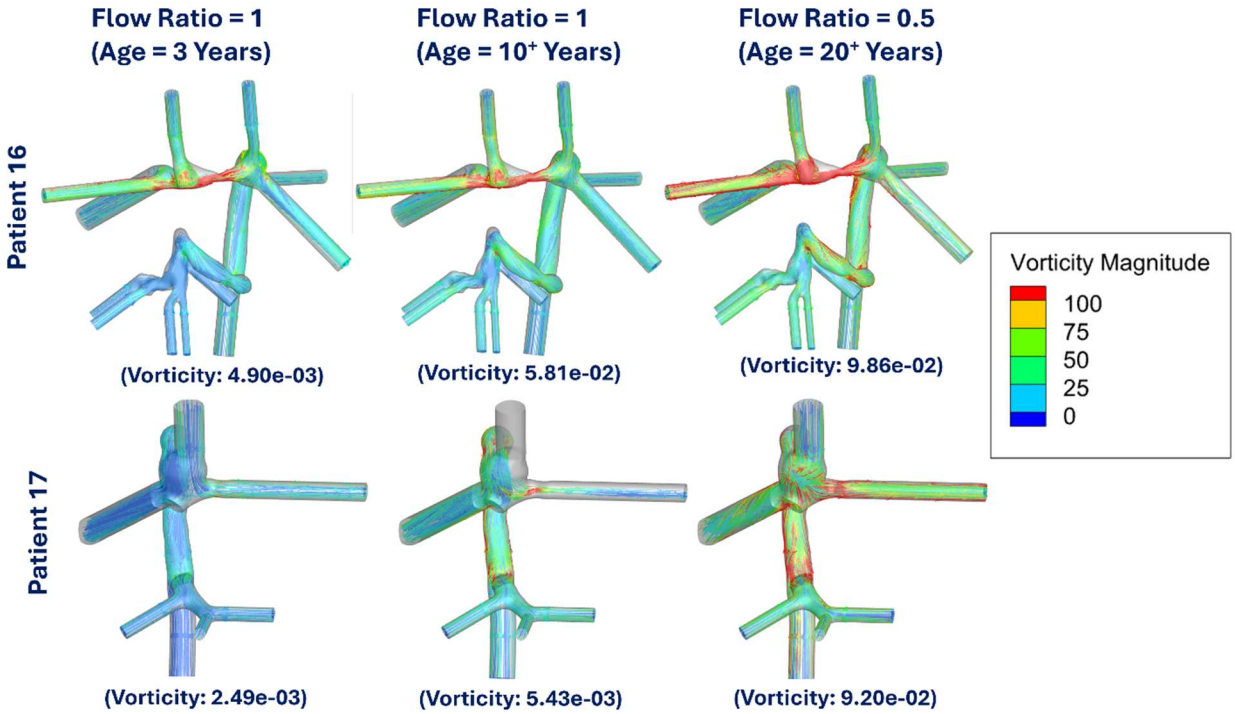

Figure S2.6 Age-related spatial variation of Vorticity with upper-to-lower body flow ratios for different patients, with corresponding value of integrated vorticity.

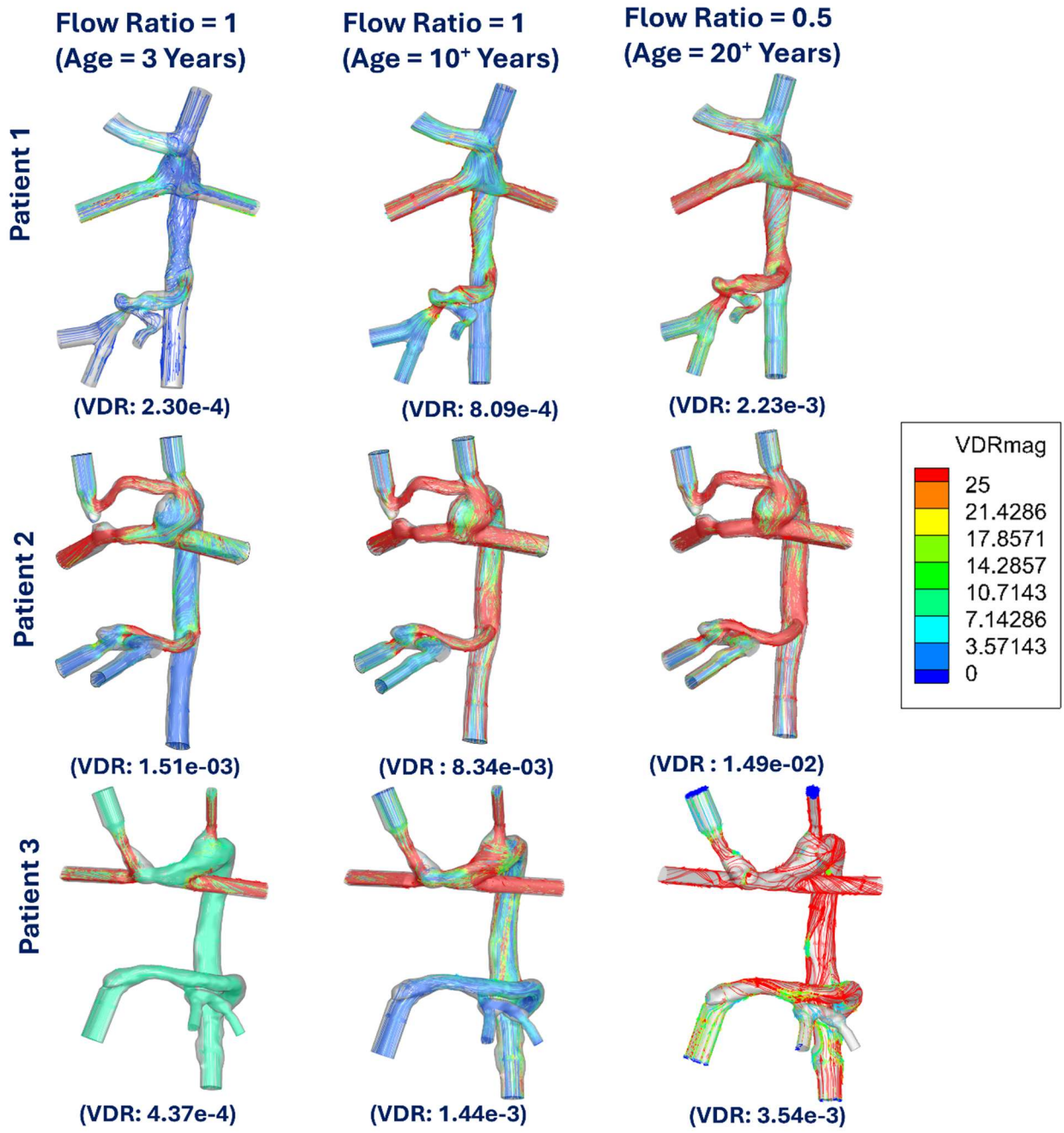

Figure S3.1 Age-related spatial variation of VDR with upper-to-lower body flow ratios for different patients, with corresponding value of integrated vorticity.

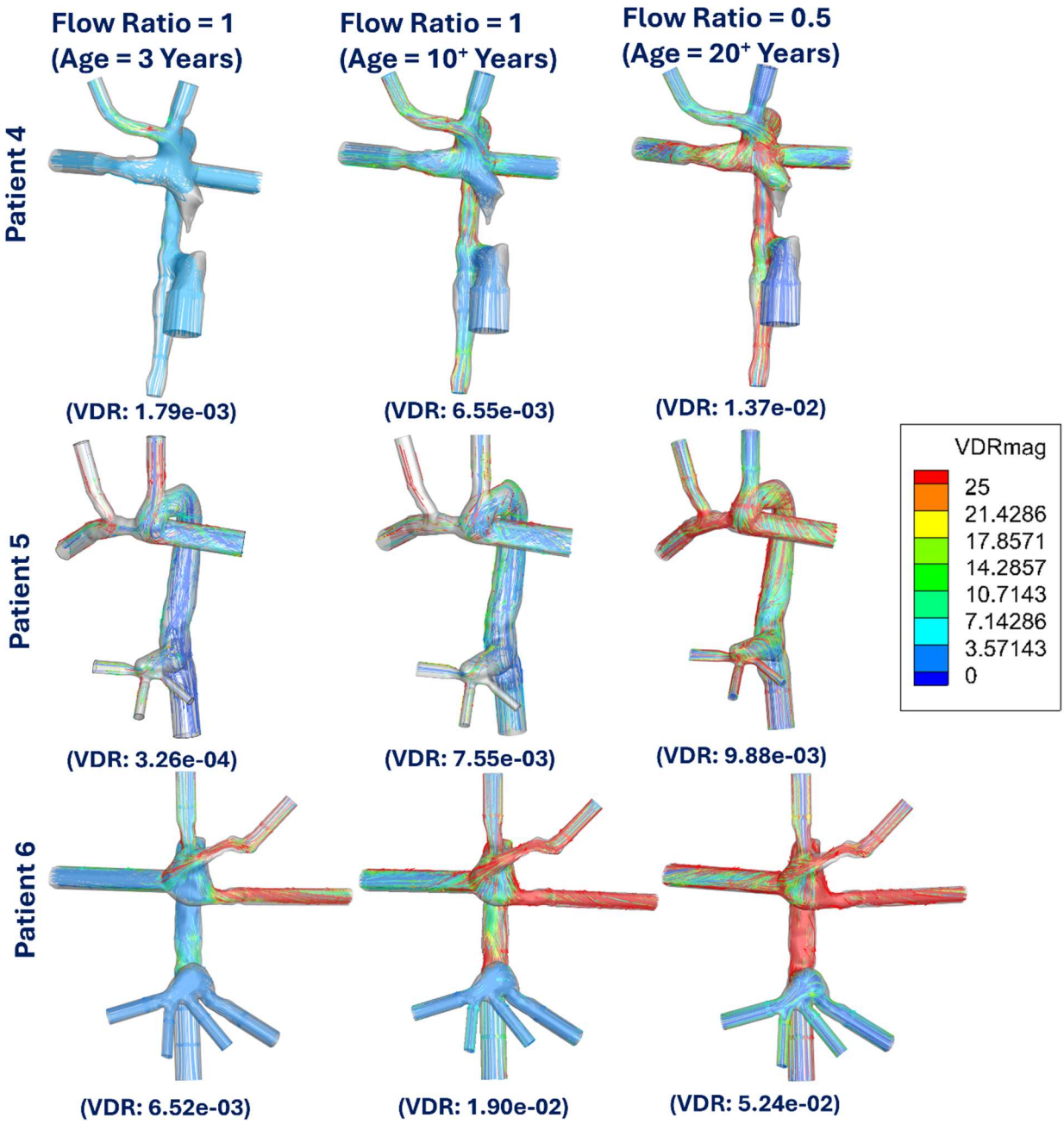

Figure S3.2 Age-related spatial variation of VDR with upper-to-lower body flow ratios for different patients, with corresponding value of integrated vorticity.

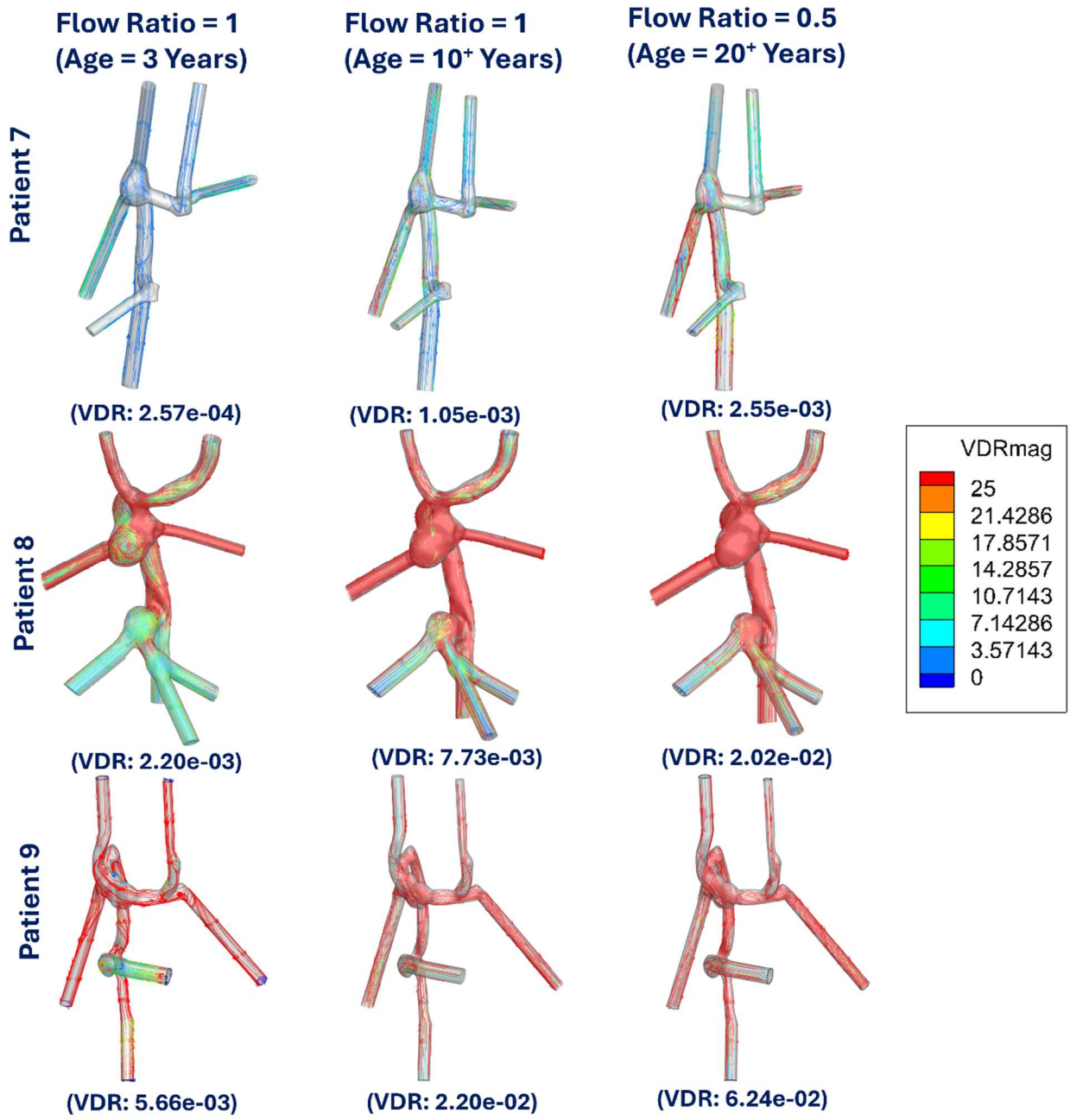

Figure S3.3 Age-related spatial variation of VDR with upper-to-lower body flow ratios for different patients, with corresponding value of integrated vorticity.

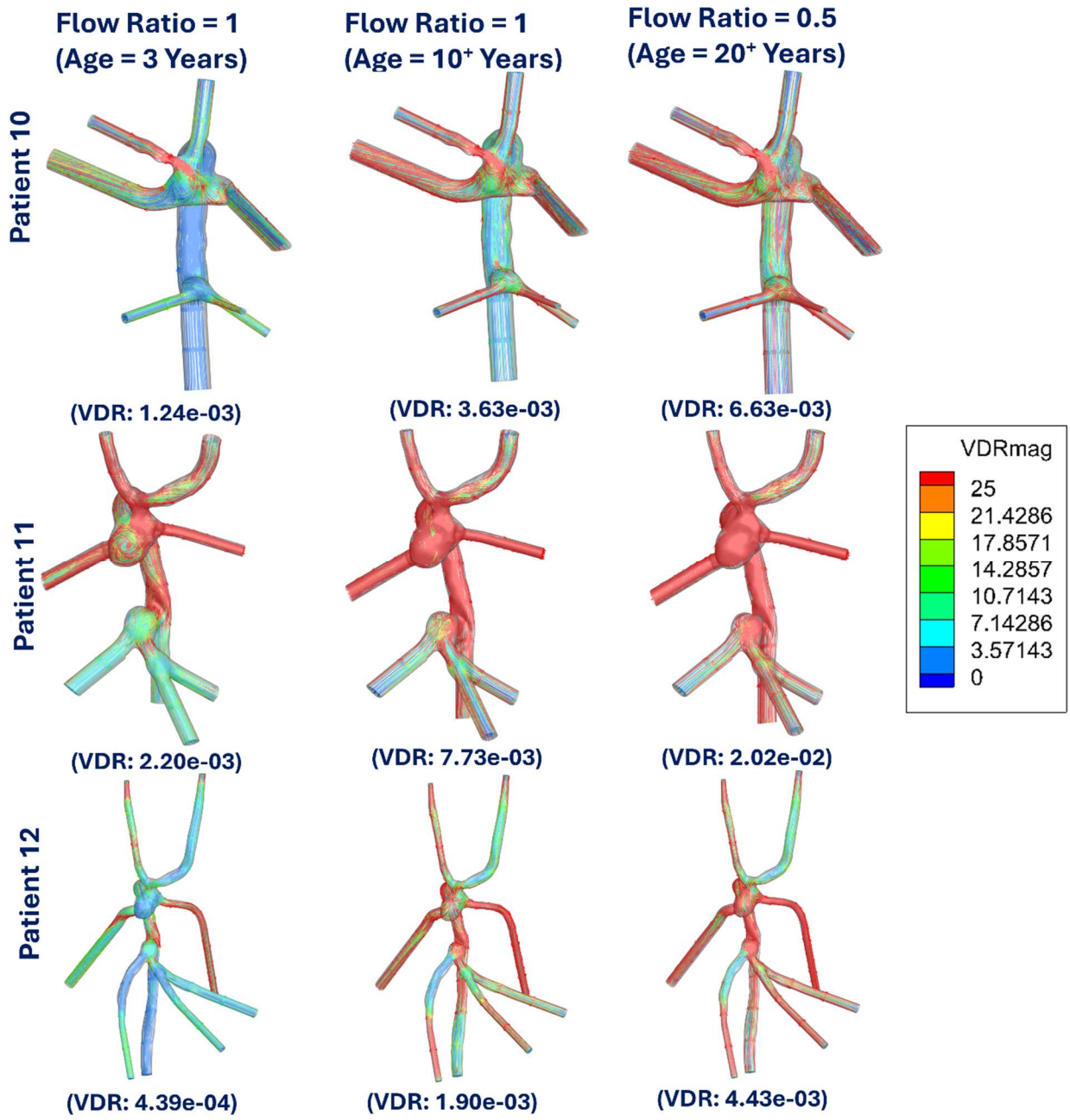

Figure S3.4 Age-related spatial variation of VDR with upper-to-lower body flow ratios for different patients, with corresponding value of integrated vorticity.

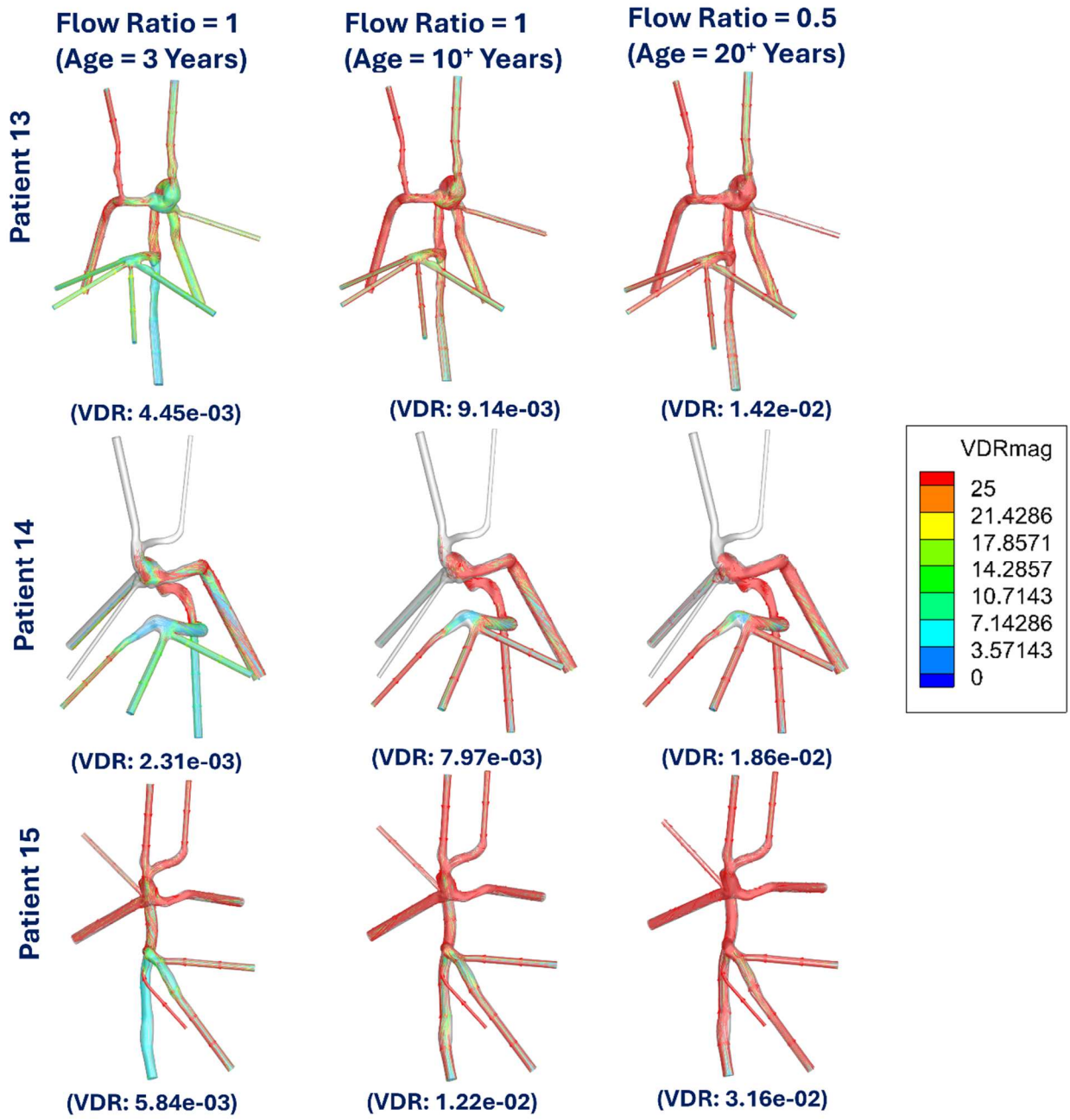

Figure S3.5 Age-related spatial variation of VDR with upper-to-lower body flow ratios for different patients, with corresponding value of integrated vorticity.

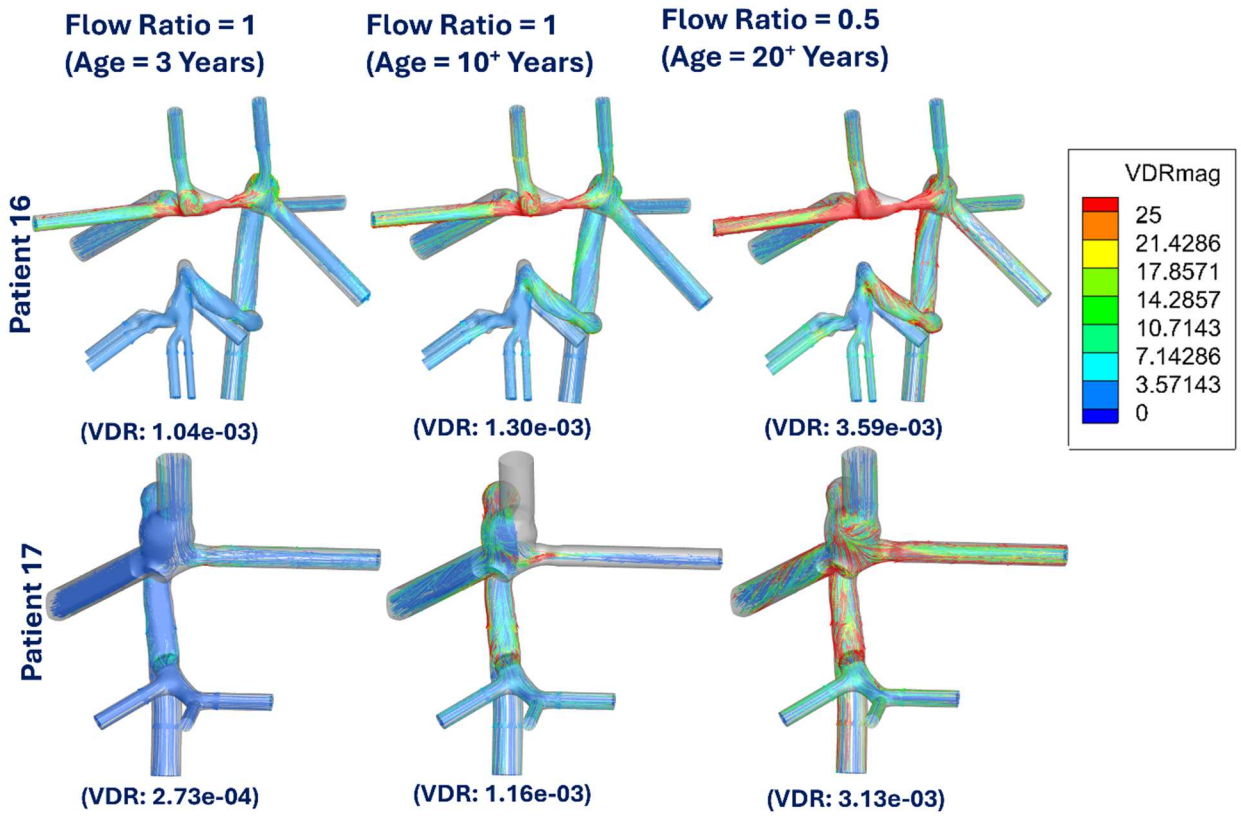

Figure S3.6 Age-related spatial variation of VDR with upper-to-lower body flow ratios for different patients, with corresponding value of integrated vorticity.

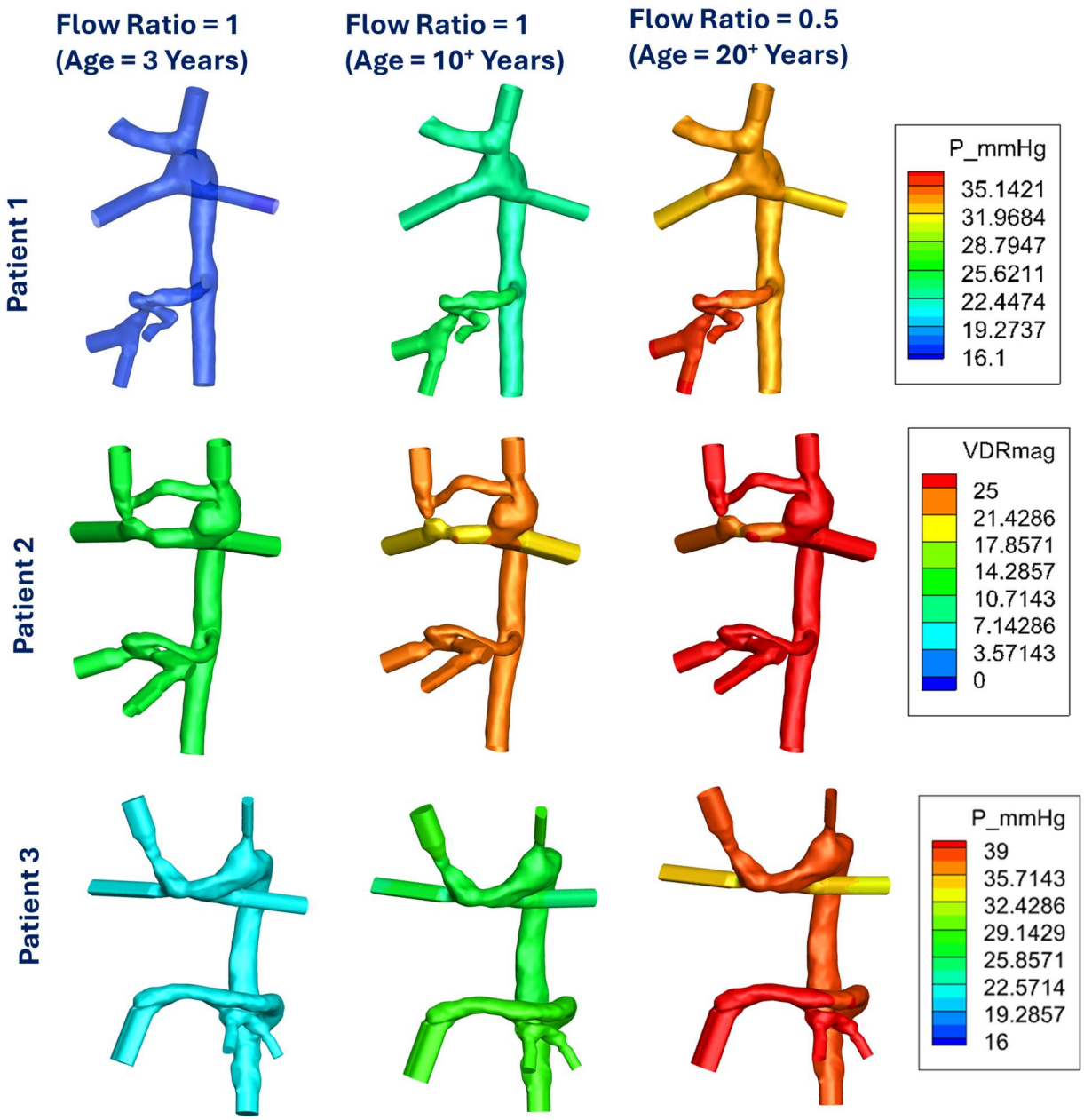

Figure S4.1 Variation of pressure distribution with age-related changes in upper-to-lower body flow ratios for different patients

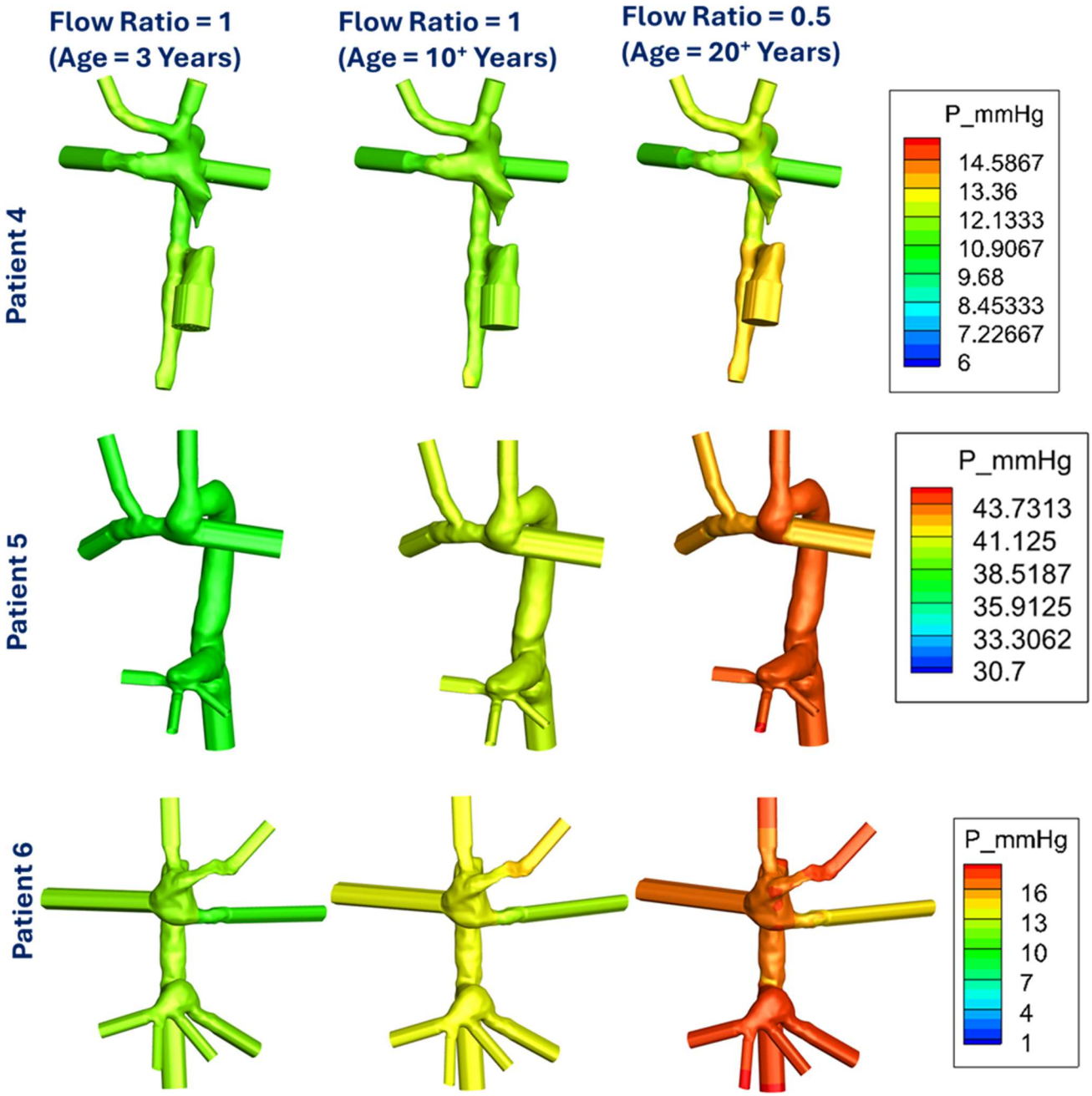

Figure S4.2 Variation of pressure distribution with age-related changes in upper-to-lower body flow ratios for different patients

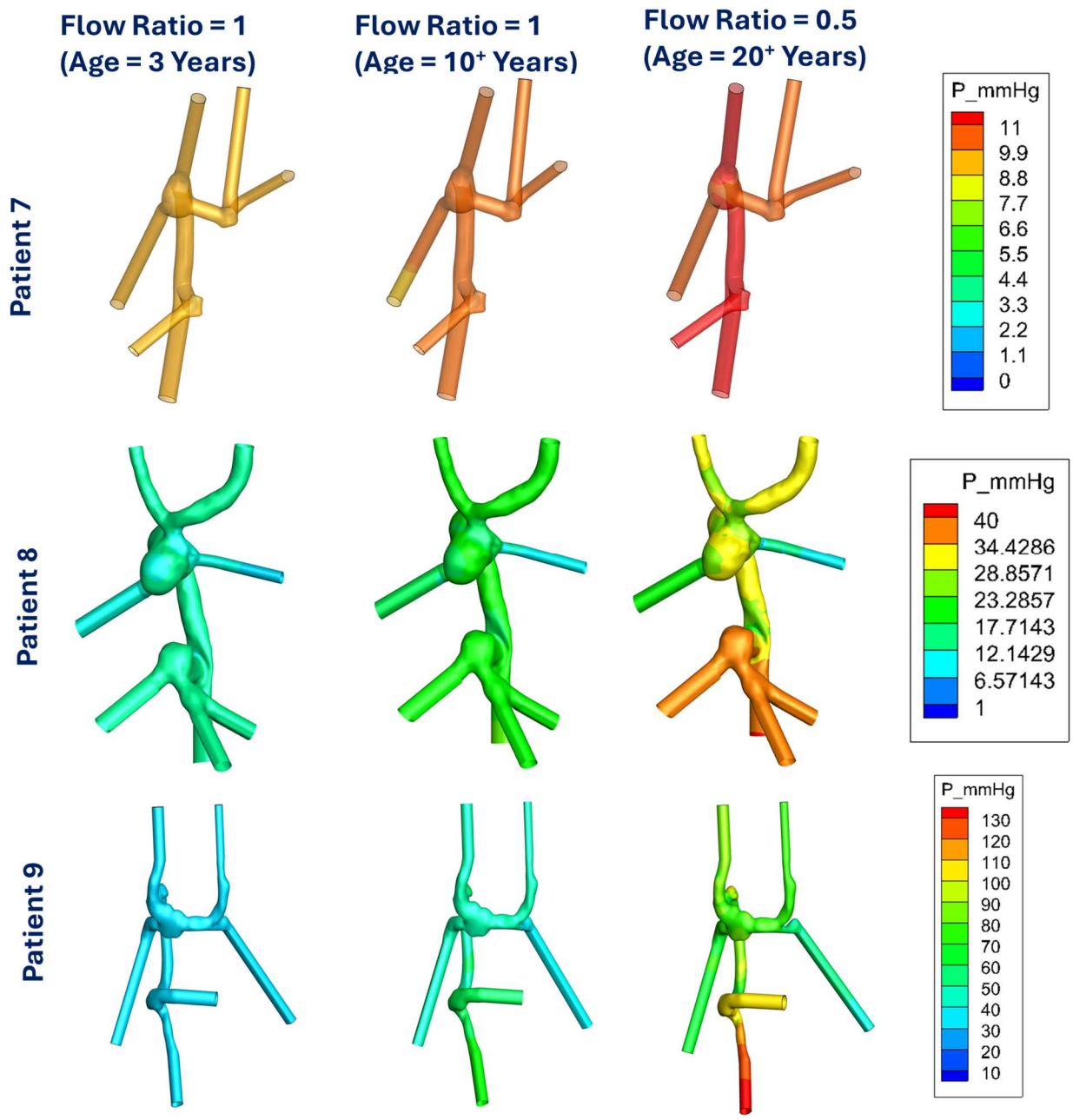

Figure S4.3 Variation of pressure distribution with age-related changes in upper-to-lower body flow ratios for different patients. Please note that Patient 9 had a constricted IVC that may have led to a high pressure distribution particularly for Age ~20 years.

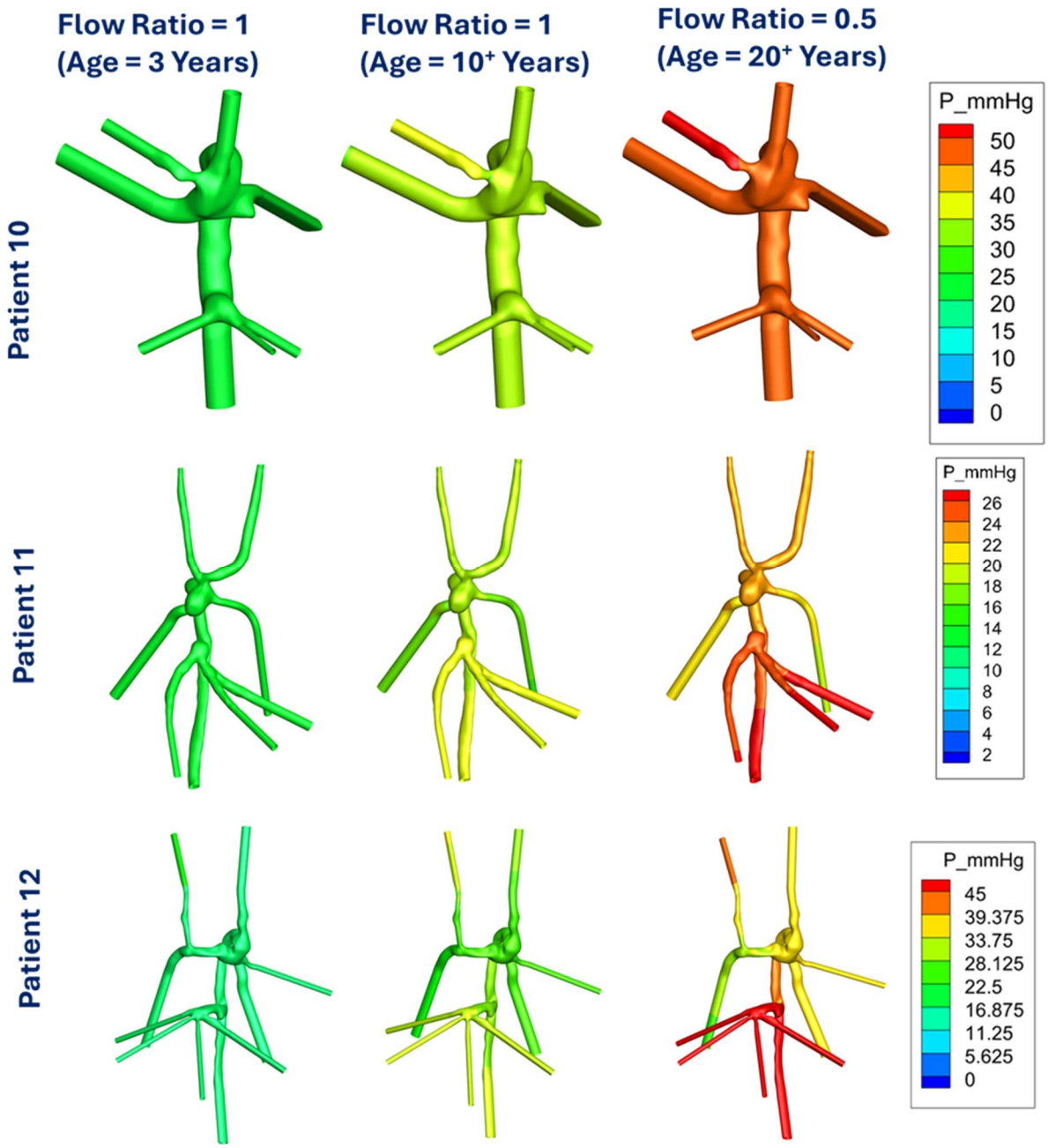

Figure S4.4 Variation of pressure distribution with age-related changes in upper-to-lower body flow ratios for different patients

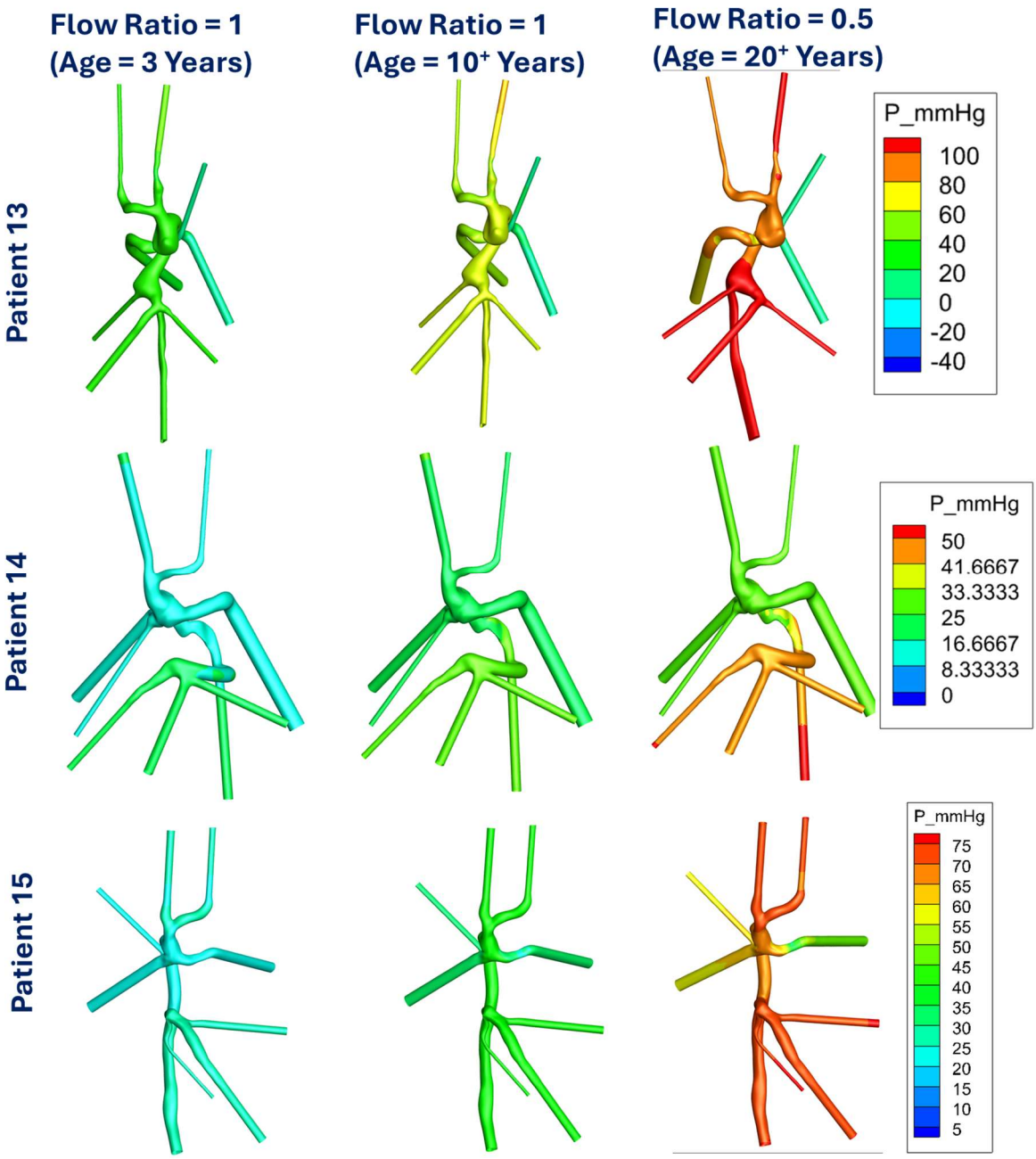

Figure S4.5 Variation of pressure distribution with age-related changes in upper-to-lower body flow ratios for different patients. Please note that Patient 13 had a constricted IVC and SVC that may have led to a high pressure distribution particularly for Age ~20 years.

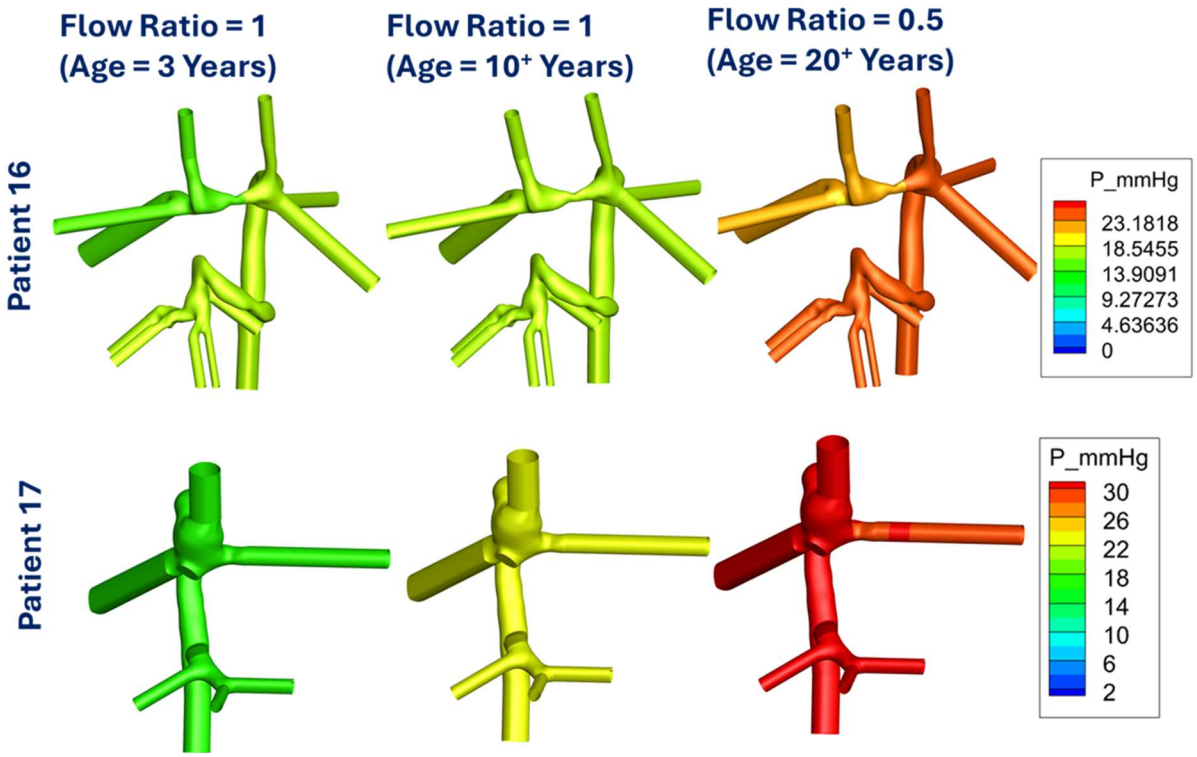

Figure S4.6 Variation of pressure distribution with age-related changes in upper-to-lower body flow ratios for different patients

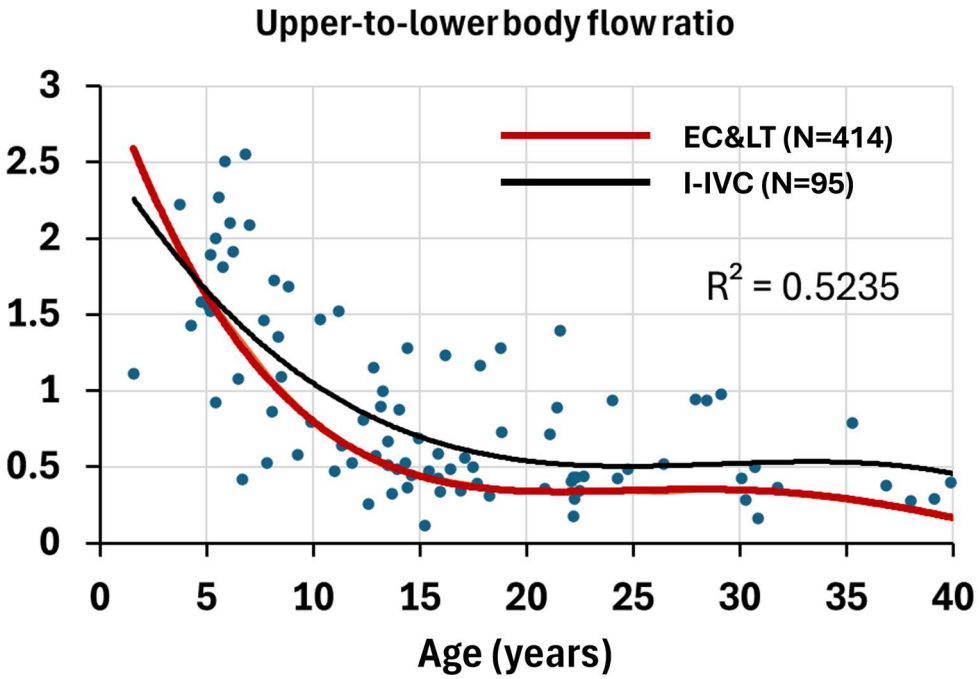

Figure S5 Comparison of Upper-to-lower body inflow ratio measured between the I-IIVC cohort (current study) and the extracardiac & lateral tunnel (EC & LT) cohort from our previous study(1). For clarity, only the regression line (in red) is shown for the EC and LT cohorts.

Supplementary Reference:

1. **Govindarajan V, Marshall L, Sahni A, Cetatoiu MA, Eickhoff EE, Davee J, St. Clair N, Schulz NE, Hoganson DM, and Hammer PE**. Impact of Age-Related Change in Caval Flow Ratio on Hepatic Flow Distribution in the Fontan Circulation. *Circ Cardiovasc Imaging* 17: e016104, 2024.